

Evidence against the wobbling nature of low-spin bands in  $^{135}\text{Pr}$ 

B.F. Lv<sup>a,b</sup>, C.M. Petrache<sup>b,\*</sup>, E.A. Lawrie<sup>c,d</sup>, S. Guo<sup>a,e</sup>, A. Astier<sup>b</sup>, K.K. Zheng<sup>a,b</sup>, H.J. Ong<sup>a,e</sup>, J.G. Wang<sup>a,e</sup>, X.H. Zhou<sup>a,e</sup>, Z.Y. Sun<sup>a,e</sup>, P.T. Greenlees<sup>f</sup>, H. Badran<sup>f</sup>, T. Calverley<sup>f,g</sup>, D.M. Cox<sup>f,h</sup>, T. Grahn<sup>f</sup>, J. Hilton<sup>f,g</sup>, R. Julin<sup>f</sup>, S. Juutinen<sup>f</sup>, J. Konki<sup>f,i</sup>, J. Pakarinen<sup>f</sup>, P. Papadakis<sup>f,g</sup>, J. Partanen<sup>f</sup>, P. Rahkila<sup>f</sup>, P. Ruotsalainen<sup>f</sup>, M. Sandzelius<sup>f</sup>, J. Sarén<sup>f</sup>, C. Scholey<sup>f</sup>, J. Sorri<sup>f,j</sup>, S. Stolze<sup>f,k</sup>, J. Uusitalo<sup>f</sup>, B. Cederwall<sup>l</sup>, A. Ertoprak<sup>l</sup>, H. Liu<sup>l</sup>, I. Kuti<sup>m</sup>, J. Timár<sup>m</sup>, A. Tucholski<sup>n</sup>, J. Srebrny<sup>n</sup>, C. Andreoiu<sup>o</sup>

<sup>a</sup> Key Laboratory of High Precision Nuclear Spectroscopy and Center for Nuclear Matter Science, Institute of Modern Physics, Chinese Academy of Sciences, Lanzhou 730000, People's Republic of China

<sup>b</sup> Université Paris-Saclay, CNRS/IN2P3, IJCLab, 91405 Orsay, France

<sup>c</sup> iThemba LABS, National Research Foundation, PO Box 722, Somerset West 7129, South Africa

<sup>d</sup> Department of Physics, University of the Western Cape, Private Bag X17, 7535 Bellville, South Africa

<sup>e</sup> School of Nuclear Science and Technology, University of Chinese Academy of Science, Beijing 100049, People's Republic of China

<sup>f</sup> University of Jyväskylä, Department of Physics, P.O. Box 35, FI-40014, University of Jyväskylä, Finland

<sup>g</sup> Oliver Lodge Laboratory, Department of Physics, University of Liverpool, Liverpool L69 7ZE, United Kingdom

<sup>h</sup> Department of Mathematical Physics, Lund Institute of Technology, S-22362 Lund, Sweden

<sup>i</sup> CERN, CH-1211 Geneva 23, Switzerland

<sup>j</sup> Sodankylä Geophysical Observatory, University of Oulu, FIN-99600 Sodankylä, Finland

<sup>k</sup> Physics Division, Argonne National Laboratory, Argonne, IL 60439, USA

<sup>l</sup> KTH Department of Physics, S-10691 Stockholm, Sweden

<sup>m</sup> Institute for Nuclear Research (Atomki-ELKH), 4001 Debrecen, Hungary

<sup>n</sup> University of Warsaw, Heavy Ion Laboratory, Pasteura 5a, 02-093 Warsaw, Poland

<sup>o</sup> Department of Chemistry, Simon Fraser University, Burnaby, BC V5A 1S6, Canada

## ARTICLE INFO

## Article history:

Received 23 August 2021

Received in revised form 24 November 2021

Accepted 13 December 2021

Available online 15 December 2021

Editor: B. Blank

## Keywords:

$\gamma\gamma\gamma$ -coincidences

Angular correlations

Particle rotor model

Wobbling bands

## ABSTRACT

The electromagnetic character of the  $\Delta I = 1$  transitions connecting the 1- to 0-phonon and the 2- to 1-phonon wobbling bands should be dominated by an  $E2$  component, due to the collective motion of the entire nuclear charge. In the present work it is shown, based on combined angular correlation and linear polarization measurements, that the mixing ratios of all analyzed connecting transitions between low-lying bands in  $^{135}\text{Pr}$  interpreted as 0-, 1-, and 2-phonon wobbling bands, have absolute values smaller than one. This indicates predominant  $M1$  magnetic character, which is incompatible with the proposed wobbling nature. All experimental observables are instead in good agreement with quasiparticle-plus-triaxial-rotor model calculations, which describe the bands as resulting from a rapid re-alignment of the total angular momentum from the short to the intermediate nuclear axis.

© 2021 The Author(s). Published by Elsevier B.V. This is an open access article under the CC BY license (<http://creativecommons.org/licenses/by/4.0/>). Funded by SCOAP<sup>3</sup>.

Wobbling motion was a topic of great interest in nuclear physics over the last years. This collective mode of excitation is considered as a clear fingerprint of the presence of stable triaxiality in a deformed rotating nucleus. Initially proposed by Bohr and Mottelson for even-even nuclei at high spin [1], the wobbling mode occurs when the three principal axes of the nuclear density distribution are unequal. Due to the triaxiality such nucleus rotates simultaneously around all of its three axes. It was demonstrated

that the approximation of such rotation with wobbling motion, where the excited rotational bands are generated by the excitation of wobbling phonons, is a good approximation at high spin.

Experimentally, the wobbling motion has been identified through the observation of  $\Delta I = 2$  rotational bands with similar moments of inertia and excitation energies increasing with the number of wobbling oscillation quanta. The most important direct evidence of the wobbling mode is obtained from the examination of the connecting  $\Delta I = 1$  transitions between bands differing by one wobbling phonon, which, due to the fact that the wobbling motion involves the entire nuclear charge, should have predominantly electric  $E2$  character.

\* Corresponding author.

E-mail address: [petrache@ijclab.in2p3.fr](mailto:petrache@ijclab.in2p3.fr) (C.M. Petrache).

The pioneering experimental evidence for nuclear wobbling motion was reported in the triaxial superdeformed  $^{161-167}\text{Lu}$  and  $^{167}\text{Ta}$  odd-even nuclei two decades ago [2–7]. In all these nuclei the wobbling bands were assigned to the  $\pi i_{13/2}$  intruder configuration with large deformation of  $\varepsilon_2 \approx 0.4$ , and the spin of the odd nucleon parallel to that of the core.

Recently, a new type of wobbling motion in odd-mass nuclei, called transverse wobbling, was proposed by Frauendorf and Dönaeu [8], in which the angular momentum of the odd nucleon is orthogonal to the angular momentum of the core. This is in contrast with the longitudinal coupling of the angular momenta of the odd nucleon and the core, accepted previously for the high-spin bands in the odd-mass Lu and Ta isotopes (see e.g. [9]). The new transverse wobbling mode was proposed for both the low-spin bands in  $^{135}\text{Pr}$ , and the high-spin bands of the odd-mass Lu isotopes [8]. This new idea opened an intense research activity which led to the publication of transverse and longitudinal wobbling bands in  $^{135}\text{Pr}$  [10,11],  $^{105}\text{Pd}$  [12],  $^{130}\text{Ba}$  [13],  $^{133}\text{La}$  [14],  $^{127}\text{Xe}$  [15],  $^{187}\text{Au}$  [16],  $^{183}\text{Au}$  [17], and  $^{136}\text{Nd}$  [18]. In particular, the 1- and 2-phonon transverse wobbling bands in  $^{135}\text{Pr}$  reported in Refs. [10,11] comprise previously observed negative-parity states without a proposed interpretation in Ref. [19]. The critical experimental evidence supporting the wobbling interpretation come from the measured magnitudes of the mixing ratios of three transitions connecting the proposed 1-phonon wobbling band to the yrast band and also of three transitions connecting the proposed two-phonon and 1-phonon wobbling bands. The magnitudes of mixing ratios extracted for these transitions from angular correlation measurement was larger than one. It is well known from the literature that the extraction of the mixing ratios of  $\Delta I = 1$  transitions from angular distribution alone yields two solutions,  $|\delta_1| > 1$  and  $|\delta_2| < 1$ , resulting from the  $\chi^2$  fit to the experimental points. This ambiguity can be solved by a linear polarization measurement. However, in the case of the wobbling bands of  $^{135}\text{Pr}$  polarization results were carried out for only two out of the six linking transitions, and in addition, as pointed out in Ref. [20], the magnitude of the measured linear polarization was not used, but only its sign, to conclude on their predominant  $E2$  character. Moreover, the polarization data for the two transitions linking the 1-phonon to the yrast band, presented in Ref. [10], are in contradiction with those of Ref. [21] published soon after Ref. [10], while performed using the same reaction and the same setup [21]. The last paper was followed by an erratum [24] which reports similar polarization results as those of Ref. [10], however some questions were raised with respect to the analysis, Ref. [23]. Considering the apparent uncertainty in the polarization data for the 1-phonon band and the lack of any polarization data for the two-phonon band, doubts on the available experimental evidence for the proposed wobbling bands remain. Therefore, a further investigation of the mixing ratios and polarization asymmetries in  $^{135}\text{Pr}$  appears as necessary to clarify the nature of the connecting transitions of the proposed wobbling bands.

Theoretically, a considerable debate about the validity of transverse wobbling motion in odd-mass nuclei is in course. The frozen approximation proposed in Ref. [8] appears unrealistic, because it leaves out the effect of the Coriolis force on the odd nucleon coupled transversely to the core [22,25,26]. Very recently, the wobbling interpretation of the low-lying yrare bands in odd-mass nuclei was questioned in Refs. [27,28]. It was shown that the transverse wobbling equations as given in Ref. [8] are not equivalent to the rotational Hamiltonian of the quasiparticle-plus-triaxial-rotor (QTR) model which describes three dimensional rotation, and do not accurately describe the excitation of wobbling quanta. As the three-dimensional rotation of a triaxial odd-mass nucleus represents in fact a precession of the total angular momentum around a

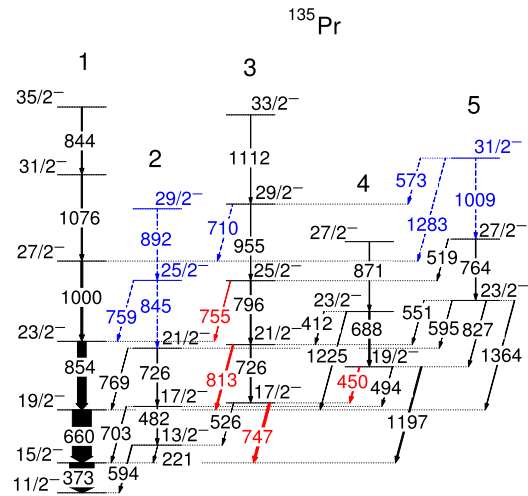


**Fig. 1.** Partial level scheme of  $^{135}\text{Pr}$  showing the negative-parity bands discussed in the present work. The transitions of interest are drawn in red, while transitions reported in previous works [19,10,11], but not observed in the present data, are drawn with dashed blue lines.

certain axis, the low-lying yrare bands in triaxial nuclei were called Tilted Precession (TiP) bands [27].

The present work concentrates on accurate measurements of the mixing ratios of the transitions connecting low-lying states in  $^{135}\text{Pr}$ , using both linear polarization and angular correlation analysis [29–31], in order to provide crucial evidence on the real nature of the low-lying excited bands in  $^{135}\text{Pr}$ .

The low-lying negative-parity bands in  $^{135}\text{Pr}$  have been investigated using the  $^{100}\text{Mo}(^{40}\text{Ar}, 1p4n)$  reaction at a bombarding energy of 152 MeV. The  $^{40}\text{Ar}$  beam was provided by the K130 Cyclotron at the University of Jyväskylä, Finland. The target was a  $0.5 \text{ mg/cm}^2$  thick self-supporting foil of enriched  $^{100}\text{Mo}$ . Excited  $^{135}\text{Pr}$  nuclei were produced with approximately 30% of the total cross section. Prompt  $\gamma$ -rays were detected by the JUROGAM II spectrometer comprising of 24 EUROGAM clover [32] and 15 EUROGAM phase one [33] Compton-suppressed germanium detectors. Approximately  $5.1 \times 10^{10}$  three and higher-fold  $\gamma$ -ray coincidence events were obtained and stored. The data were sorted into coincidence  $\gamma$ - $\gamma$  matrices and  $\gamma$ - $\gamma$ - $\gamma$  cubes, and analyzed using the RADWARE [34,35] and GASPWARE packages [36].

The partial level scheme of  $^{135}\text{Pr}$  shown in Fig. 1 is constructed using the relative intensity ( $I_\gamma$ ) balance and coincidence relationships of the  $\gamma$ -ray transitions. It is in agreement with Refs. [21,19], but in contrast with the grouping of the 827-, 764- and 1009-keV transitions as one band, which was interpreted as two phonon wobbling bands in Ref. [11]. These three transitions do not correspond to increasing  $\gamma$ -ray energy, as expected for a rotational band. Therefore the second excited  $19/2^-$  state in  $^{135}\text{Pr}$  is assigned here as the band head of the new band 4, consisting of the 688- and 871-keV transitions which are much stronger than the 827-keV transition (see Fig. 2(a) in the supplementary material [37]), and have the approximate  $I(I+1)$  energy dependence of a rotational band. If one considers the 1009-keV transition reported in Ref. [11] but not observed in the present work, the 764-keV transition is the first transition of a possible new rotational band, band 5, built on the third excited  $23/2^-$  state in  $^{135}\text{Pr}$ , while the 827-keV transition links this band to band 4. The multipolarity and the mixing ratios of the  $\gamma$ -ray transitions were established based on two-point angular distribution (anisotropy) ratios  $R_{ac}$  [30,38] and linear polarization measurements [39,40]. The complete experimental information on levels,  $\gamma$ -ray transitions, and experimental techniques are presented in the supplementary material [37].

Bands 1 and 2 reported in Ref. [19] were interpreted as the favored and unfavored signatures of the lowest-energy  $\pi h_{11/2}$  orbital. In a more recent work, band 2 was extended to higher spin by one transition. In the same work, some previously observed transitions were assigned to band 3 [11]. Based on angular distribution measurements, mixing ratios with magnitudes larger than one were derived for the 747-, 813-, and 755-keV transitions linking band 3 to band 1, and with magnitude smaller than one for the 594-keV transition linking band 2 to band 1 [10]. The positive values of the measured linear polarization for the 747- and 813-keV transitions were considered as confirming the larger-than-one values of the deduced mixing ratios. Based on these experimental results band 3 was interpreted as a 1-phonon wobbling band, while band 2 was assigned as a signature partner of band 1. In another work [11], angular distribution and DCO-like measurements only were used to extract mixing ratios for the 450-, 551-, and 519-keV transitions, which were assigned as linking the two- and the 1-phonon wobbling bands. The extracted larger-than-one magnitudes were considered as a deciding proof for the proposed wobbling phonon interpretation.

However, as pointed out above, the  $\chi^2$  fit of the angular distribution data usually yields two solutions for the mixing ratio,  $|\delta_1| > 1$  and  $|\delta_2| < 1$ . For instance, Fig. 2 shows the angular distribution data for the 747-, 813- and 450-keV transitions from Refs. [10,11], together with the fitted curves yielding  $|\delta_1| > 1$  (the blue dashed line [10,11]) and  $|\delta_2| < 1$  (the red solid line [20]). Therefore, both solutions  $\delta_1$  and  $\delta_2$  are possible. In order to select the correct one, linear polarization measurements are needed. However, out of the six linking transitions in  $^{135}\text{Pr}$  for which the  $\delta_1$  solution was selected, linear polarization data are available for only two, the 747- and the 813-keV transitions. Furthermore, the magnitude of the measured linear polarization was not used to select the correct solution of  $\delta$ , but it was assumed that the positive sign of the polarization confirms the solution with larger magnitude. However, the positive sign does not necessarily select the  $|\delta| > 1$  values [40], as also pointed out in Ref. [20].

In the present work, new mixing ratios for the 747-, 813-keV, and 450-keV transitions are determined from complementary measurements of linear polarization  $P$  and angular distribution ratio  $R_{ac}$ , see Figs. 2(b), 2(d), 2(f) and Table 1. As illustrated in Fig. 2, the  $P - R_{ac}$  analysis allows the extraction of the mixing ratios  $\delta$  for the 747-, 813- and 450-keV transitions of  $-0.47^{+9}_{-22}$ ,  $-0.37^{+10}_{-14}$ , and  $-0.31^{+10}_{-13}$ , respectively. The smaller-than-one absolute mixing ratios of the three transitions are in contradiction with the larger-than-one mixing ratios reported in Ref. [10,11], and indicate predominant magnetic character at the level of 82%, 88% and 91% for the 747-, 813-, and 450-keV transitions, respectively. The higher lying 755-keV connecting transition is too weak to allow the extraction of polarization asymmetry (as in a previous work [10]). However its  $R_{ac}$  ratio is very similar to that of the 813-keV transition, suggesting similar solutions for  $\delta$ .

The predominant magnetic character of the 747- and 813-keV transitions connecting bands 3 and 1 is therefore in distinct disagreement with the predominant electric character deduced in Ref. [10] and incompatible with the proposed 1-phonon wobbling interpretation of band 3. As an additional test, let us assume that band 3 is a 1-phonon wobbling excitation with respect to band 1. In this case, the  $B(E2; 747)/B(E2; 526)$  reduced transition probability to band 1 would be large, while  $B(E2; 526)$  to band 2 would be negligible, as it would correspond to a decay to the signature partner band 2, which is forbidden. The presently measured ratio  $B(E2; 747)/B(E2; 526) = 0.7^{+0.7}_{-0.5}$  indicates similar strengths of the two transitions, and is therefore in disagreement with the wobbling interpretation of band 3. The predominant magnetic character of the 450-keV transition is also inconsistent with the previously proposed interpretation [11], which described it as a link

**Table 1**

The experimental polarization value  $P$ , angular correlation ratios  $R_{ac}$ , mixing ratios  $\delta$ , and ratios of out-of-band and in-band reduced transition probabilities of the connecting transitions between bands 3 and 1, and between bands 4 and 3.

$E_\gamma$ (keV)	$P$	$R_{ac}$	$\delta$	$\frac{B(M1)_{out}}{B(E2)_{in}}$	$\frac{B(E2)_{out}}{B(E2)_{in}}$
747.3	$0.04^{+8}_{-13}$	0.37(4)	$-0.47^{+9}_{-22}$		
813.2	$-0.03^{+5}_{-12}$	0.48(6)	$-0.37^{+10}_{-14}$	0.4(3)	0.12(8)
755.1		0.50(6)			
450.2	$-0.07^{+9}_{-10}$	0.49(4)	$-0.31^{+10}_{-13}$		

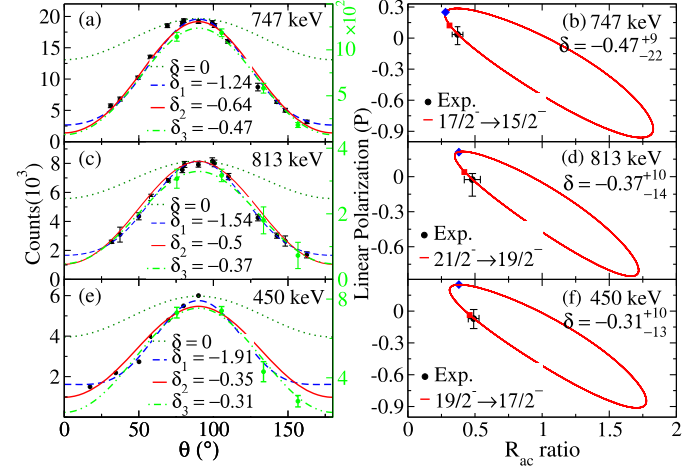


**Fig. 2.** (a), (c), (e) Angular distribution reported in Refs. [10,11] with fits corresponding to the previously reported  $|\delta| > 1$  and  $|\delta| = 0$  values, as well as with our best fit of the same data reported in Refs. [10,11] which correspond to  $|\delta| < 1$  values. The angular distribution from the present work is also shown with green color, with the y-axis on the right side. (b)(d)(f) Linear polarization ( $P$ ) as a function of  $R_{ac}$  for the 747-, 813-, and 450-keV transitions connecting bands 3 and 4 to band 1, respectively. The experimental values are given with error bars. The values indicated with blue-diamond and red-square represent  $|\delta| > 1$  and  $|\delta| < 1$  solutions indicated in panels (a), (c) and (e), respectively. The  $\delta$  values extracted from the present data are also given.

between a 2- and a 1-phonon wobbling bands. Therefore, according to presented measurements, the second  $19/2^-$  state in  $^{135}\text{Pr}$  does not have a wobbling nature.

Prior to this work, the negative-parity states in  $^{135}\text{Pr}$  have been investigated using different models: the QTR model, tilted axis cranking (TAC) mean-field calculations, the triaxial projected shell model (TPSM), and constrained triaxial covariant density functional theory, as well as the particle rotor model [8,10,11]. Band 1 was assigned to the  $\pi h_{11/2}$  configuration, band 2 was considered as the signature partner of band 1, and bands 3 and the levels of band 5 together with the  $19/2^-$  level of band 4 were interpreted as 1-phonon and 2-phonon transverse wobbling bands, respectively. The experimental results described above and the theoretical calculations reported in the following do not support the proposed transverse wobbling nature of these bands.

In order to explore the nature of the five bands discussed in the present work we performed QTR calculations [41]. The QTR model predicts rotational bands that result from the coupling of rotational and single-particle components, as shown in Fig. 3. The sketch in panel (a) illustrates the rotation of a triaxial even-even core, where the nucleus can rotate around its 3 axes [3-dimensional (3D) rotation]. The moments of inertia around the three axes are usually described as a function of the  $\gamma$  deformation within the irrotational-flow model, a dependence that was recently supported by empirical data [42]. As the moment of inertia along the intermediate axis is largest for any value of  $\gamma$ , the rotation around this axis,  $R_i$ , corresponds to lowest excitation energy and is favored. Therefore states based on such rotation form the ground-

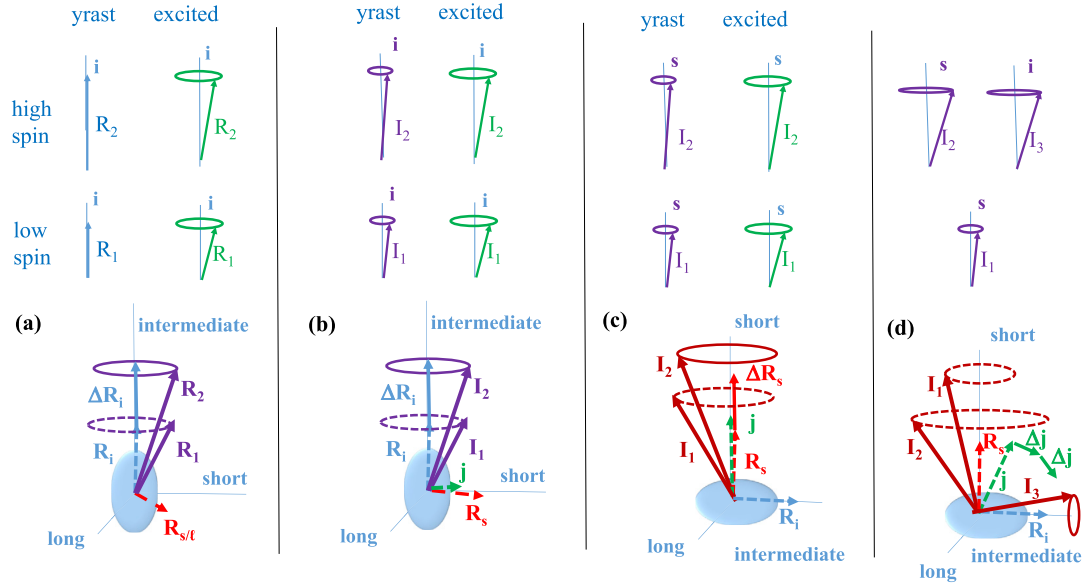


**Fig. 3.** The panels illustrate the different excitation mechanisms for rotating triaxial (a) even-even, and (b-d) odd-mass nuclei. The angular momentum generated in the yrast and in excited bands, and at low ( $I_1$ ) and high ( $I_2, I_3$ ) spins, is sketched for a favored rotation around the intermediate axis in panels (a) and (b), around the short axis in panel (c), and for single-particle excitation, where the odd  $h_{11/2}$  proton is excited to higher-energy orbitals from the same shell in panel (d). The rotational angular momenta along the intermediate,  $R_i$ , and the short,  $R_s$ , and in the short-long axes plane,  $R_{s/l}$ , are shown together with the corresponding total angular momenta  $I$ , and single-particle angular momenta  $j$ . The yrast band band is generally composed by favored rotations, along the intermediate axis for (a), and (b), and along the short axis for (c). In addition to the favored rotations, unfavored rotations can also exist, leading to excited bands which involve one or several units of unfavored rotation which tilts the total angular momentum away from the axis of precession. The single-particle excitations sketched in panel (d) lead to gradual realignment of the single-particle and total angular momenta from the short to the intermediate axes.

state band in even-even triaxial nuclei, as illustrated in Fig. 3(a). Excited bands, (called in the model  $\gamma$  bands), are generated by adding unfavored rotational angular momentum in the plane of the short and long nuclear axes,  $R_{s/l}$ . These additional angular momenta generate a tilt of the total rotational angular momentum away from the intermediate axis, as shown in Fig. 3(a). The motion around the intermediate axis is similar to the precession of a rotating top around the vertical direction.

In odd-mass nuclei this 3D rotational angular momentum is coupled with the angular momentum of the valence nucleon. The single-particle angular momentum,  $j$ , is considered as initially aligned along the short nuclear axis, as expected for the  $h_{11/2}$  rotational bands in  $^{135}\text{Pr}$  in which the odd-proton lies near the lowest-energy  $h_{11/2}$  orbital. In this case the excitation energies of the nuclear states can result from three different excitation mechanisms, e.g.:

(i) rotation around the intermediate axis,  $R_i$ , which corresponds to low excitation energy, because it occurs around the axis with largest moment of inertia, illustrated in Fig. 3(b). When this mode of excitation is favored the angular momentum in the yrast band is generated by  $R_i$ , while for the excited band there is an additional one unit of  $R_s$ , which tilts the total angular momentum away from the intermediate axis.

(ii) rotation around the short nuclear axis,  $R_s$ , which may become favored as its energy is lowered additionally by a Coriolis interaction term proportional to  $\langle 1 \cdot j \rangle$ , see Fig. 3(c). As this scalar product is large when the rotational and the single-particle angular momenta are parallel to each other, it can lower significantly the energy of rotational states with  $R_s$  rotation. When this mode of excitation is favored the angular momentum in the yrast band is generated by  $R_s$ , while the excited band comprises an one unit of  $R_i$ , tilting the total angular momentum away from the short axis.

(iii) single-particle excitations, illustrated in Fig. 3(d). The proton Fermi level for  $^{135}\text{Pr}$  lies near the lowest-energy  $\pi h_{11/2}$  Nilsson orbital. The calculations suggest that the two  $\pi h_{11/2}$  Nilsson orbitals with lowest energies correspond to projections of the single-

particle orbital momentum of  $\Omega_s \approx 11/2$  and  $\approx 9/2$  along the short axis, while for the next two  $\pi h_{11/2}$  orbitals the angular momentum is predominantly aligned along the intermediate axis. Therefore single-particle excitations correspond to gradual re-alignment of the single-particle angular momentum, (and consequently of the total angular momentum), toward the intermediate axis, as illustrated in Fig. 3(d). Therefore the calculated nuclear states for the rotational bands in  $^{135}\text{Pr}$  represent a competition between these three modes of excitation.

If the calculated lowest-energy states are associated with type (ii) excitations, the higher-spin states are formed by increasing  $R_s$ , and the total angular momentum precesses around the short nuclear axis, as shown in Fig. 3(c). The rotational angular momentum  $R_i$  that tilts the total angular momentum away from the short axis of precession was approximated by harmonic vibrations and associated with excitations of wobbling phonons in Ref. [8]. The rotational bands were interpreted as wobbling bands. The wobbling phonon excitation, as a collective excitation, corresponds to large  $B(E2)$  strength, thus the corresponding transitions linking the wobbling bands have mixing ratios with large magnitude.

In previous works, the experimentally measured mixing ratios of the transitions linking the assigned 1- and 0-phonon wobbling bands, and 2- and 1-phonon wobbling bands had large magnitudes, which was interpreted as supporting the proposed wobbling nature of the bands [8,10,11]. In those works, the adopted input parameters of the QTR calculations were chosen to favor the precession around the short nuclear axis, in order to prevent a “too early a collapse of the transverse wobbling regime” [10]. The input value of the moment of inertia along the short axis was therefore increased, which lowered the excitation energy for  $R_s$  rotations. In addition, the single-particle angular momentum was “frozen” along the short nuclear axis, thus the competing mode of single-particle excitations was excluded from the calculations. With these specific constrains the QTR calculations predicted rotational bands in which the total angular momentum precessed around the short



nuclear axis for the whole spin range of the bands, as illustrated in Fig. 3(c).

Our experimental measurements yielded  $|\delta| < 1$  mixing ratios, which is in contrast with the previous experimental results of Refs. [10,11], and with the anticipated  $|\delta| > 1$  mixing ratios for bands with wobbling nature [8]. It then becomes particularly interesting to explore the competition of the three above mentioned excitation mechanisms within QTR calculations with standard input parameters, where the input parameters are not set to favor a specific type of excitation. In the following we present our QTR calculations with standard input parameters, including irrotational-flow moments of inertia and free (that is “unfrozen”) single-particle angular momentum. For easier comparison with the results of Refs. [8,10,11], we use the same deformation parameters  $\varepsilon_2 = 0.16$  and  $\gamma = 26^\circ$ . Additional details on the input parameters and the calculations are given in the supplementary material [37].

Five rotational bands lying at very similar excitation energies, in particular at high spin, were observed experimentally. The excitation energies of the calculated rotational bands agree well for bands 1, 3, and 4, but overestimate those of bands 2 and 5, to a larger extent at high spin. The larger energy spacing between the calculated bands at high spin can be caused by several factors, for instance by the interaction between the observed 1- and 3-quasiparticle bands, which results in lowering of the excitation energies of the experimentally observed 1-quasiparticle bands, or by the model assumption that all bands are described with the same moments of inertia.

The present QTR calculations suggest that all rotational bands are strongly affected by single-particle excitations (sketched in Fig. 3(d)). For all bands there is a rapid re-alignment of the single-particle angular momentum from the short to the intermediate axis. Simultaneously, the orientation of the total angular momentum changes toward the intermediate axis. The predicted rotational bands are associated with different relative components of the three types of excitations illustrated in panels (b-d) of Fig. 3, but they all undergo a re-alignment of the single-particle and of the total angular momenta toward the intermediate axis. This is in contrast with the previous QTR calculations [10,11], where this mode of excitation was excluded from the calculations and the bands were associated with precession of the total angular momentum around the short axis for the observed spin range. More details about the nature of each rotational band can be found in the supplementary material [37].

It is interesting to note that the re-alignment of the single-particle and of the total angular momenta proceeds simultaneously as a function of spin, as indicated by the almost constant expectation values of the projection of the single-particle angular momentum along the direction of the total angular momentum,  $j_{\parallel} = \langle I \cdot j \rangle / |I|$ , see Fig. 4. The value of  $j_{\parallel}$  is very close to the maximum  $j_{\parallel, \max} = 5.5$ , showing the nearly complete parallel orientation of the two angular momenta.

The present experimental data on the mixing ratios of the linking transitions between bands 3 and 1, (previously interpreted as 1- and 0-phonon wobbling bands), and on the corresponding  $B(E2)_{\text{out}}/B(E2)_{\text{in}}$  reduced transition probability ratios, are compared with the present calculations in Fig. 4. There is a very good agreement. It should be noted that the selected  $|\delta_1| > 1$  mixing ratios in Ref. [10] are in disagreement with the present experimental results and calculations. On the other hand, the selection of the second solution,  $|\delta_2| < 1$ , from the data of Ref. [10], would be in good agreement with the calculations, as shown in Fig. 4(d).

In summary, the present work reports new data on  $^{135}\text{Pr}$ , in particular the mixing ratios deduced from a combined polarization and angular distribution measurements, for three linking transitions between the previously proposed 1- and 2-phonon wobbling bands and the yrast band. The deduced absolute values of the mix-

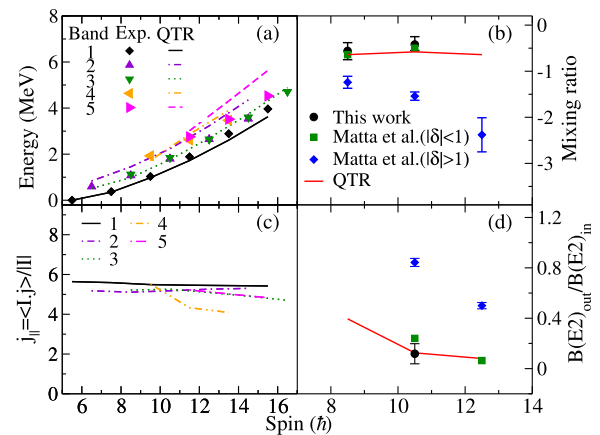


**Fig. 4.** (a) Experimental (symbols) and present QTR (lines) calculated results for the excitation energies of bands 1 to 5 in  $^{135}\text{Pr}$ . (b) Present experimental and QTR mixing ratios for the 747- and 813-keV transitions linking bands 3 and 1. For comparison, also the results of Matta et al. [10] for  $|\delta| > 1$  (blue diamond) and  $|\delta| < 1$  (green square) are shown. (c) Calculated projection of the single-particle angular momentum along the direction of the total angular momentum  $j_{\parallel} = \langle I \cdot j \rangle / |I|$  for the five bands. (d) Transition probability ratios obtained from this work (filled-circle) for the 813-keV ( $21/2^- \rightarrow 19/2^-$ ) out-of-band and 726-keV ( $21/2^- \rightarrow 17/2^-$ ) in-band transitions compared with the present QTR calculations (red line), and to the results of Matta et al. [10] for  $|\delta_1| > 1$  (blue diamond) and  $|\delta_1| < 1$  (green square).

ing ratios are all smaller than one, suggesting predominant M1 character, thus excluding the 1- and 2-phonon wobbling nature. The results of extensive QTR calculations are in good agreement with the experimental data, and indicate that the bands are tilted precession bands based on the  $\pi h_{11/2}$  configuration.

#### Declaration of competing interest

The authors declare that they have no known competing financial interests or personal relationships that could have appeared to influence the work reported in this paper.

#### Acknowledgements

This work has been supported by the Special Research Assistant Project of the Chinese Academy of Sciences; by the Strategic Priority Research Program of Chinese Academy of Sciences (Grant No. XDB34000000); by the Academy of Finland under the Finnish Centre of Excellence Programme (2012-2017); by the EU 7th Framework Programme Project No. 262010 (ENSAR); by the National Research Foundation of South Africa (Grants No. 116666 and No. 109134), and by the French Ministry of Foreign Affairs and the Ministry of Higher Education and Research, France (PHC PROTEA Grant No. 42417SE); by the National Research, Development and Innovation Fund of Hungary (Project No. K128947), as well as by the European Regional Development Fund (Contract No. GINOP-2.3.3-15-2016-00034); by the Polish National Science Centre (NCN) Grant No. 2013/10/M/ST2/00427; by the Swedish Research Council under Grant No. 621-2014-5558. The use of germanium detectors from the GAMMAPOOL is acknowledged. I.K. was supported by National Research, Development and Innovation Office-NKFIH, contract number PD 124717.

#### Appendix A. Supplementary material

Supplementary material related to this article can be found online at <https://doi.org/10.1016/j.physletb.2021.136840>.

#### References

- [1] A. Bohr, B.R. Mottelson, *Nuclear Structure*, vol. I, Benjamin, New York, 1975.

- [2] P. Bringel, et al., Evidence for wobbling excitation in  $^{161}\text{Lu}$ , *Eur. Phys. J. A* 24 (2005) 167–172, <https://doi.org/10.1140/epja/i2005-10005-7>.
- [3] S.W. Ødegård, et al., Evidence for the wobbling mode in nuclei, *Phys. Rev. Lett.* 86 (2001) 5866–5869, <https://doi.org/10.1103/PhysRevLett.86.5866>.
- [4] D.R. Jensen, et al., Evidence for second-phonon nuclear wobbling, *Phys. Rev. Lett.* 89 (2002) 142503, <https://doi.org/10.1103/PhysRevLett.89.142503>.
- [5] G. Schönwaßer, et al., One- and two-phonon wobbling excitations in triaxial  $^{165}\text{Lu}$ , *Phys. Lett. B* 552 (1) (2003) 9–16, [https://doi.org/10.1016/S0370-2693\(02\)03095-2](https://doi.org/10.1016/S0370-2693(02)03095-2), <http://www.sciencedirect.com/science/article/pii/S0370269302030952>.
- [6] H. Amro, et al., The wobbling mode in  $^{167}\text{Lu}$ , *Phys. Lett. B* 553 (3) (2003) 197–203, [https://doi.org/10.1016/S0370-2693\(02\)03199-4](https://doi.org/10.1016/S0370-2693(02)03199-4), <http://www.sciencedirect.com/science/article/pii/S0370269302031994>.
- [7] D.J. Hartley, et al., Wobbling mode in  $^{167}\text{Ta}$ , *Phys. Rev. C* 80 (2009) 041304, <https://doi.org/10.1103/PhysRevC.80.041304>.
- [8] S. Frauendorf, F. Dönau, Transverse wobbling: a collective mode in odd-*a* triaxial nuclei, *Phys. Rev. C* 89 (2014) 014322, <https://doi.org/10.1103/PhysRevC.89.014322>.
- [9] I. Hamamoto, *Phys. Rev. C* 65 (2002) 044305, <https://doi.org/10.1103/PhysRevC.65.044305>.
- [10] J.T. Matta, et al., Transverse wobbling in  $^{135}\text{Pr}$ , *Phys. Rev. Lett.* 114 (2015) 082501, <https://doi.org/10.1103/PhysRevLett.114.082501>.
- [11] N. Sensharma, et al., Two-phonon wobbling in  $^{135}\text{Pr}$ , *Phys. Lett. B* 792 (2019) 170–174, <https://doi.org/10.1016/j.physletb.2019.03.038>, <http://www.sciencedirect.com/science/article/pii/S0370269319301959>.
- [12] J. Timár, et al., Experimental evidence for transverse wobbling in  $^{105}\text{Pd}$ , *Phys. Rev. Lett.* 122 (2019) 062501, <https://doi.org/10.1103/PhysRevLett.122.062501>.
- [13] Q.B. Chen, S. Frauendorf, C.M. Petrache, Transverse wobbling in an even-even nucleus, *Phys. Rev. C* 100 (2019) 061301, <https://doi.org/10.1103/PhysRevC.100.061301>.
- [14] B. Subhagata, et al., Longitudinal wobbling in  $^{133}\text{La}$ , *Eur. Phys. J. A* 55 (2019) 159, <https://doi.org/10.1140/epja/i2019-12856-5>.
- [15] S. Chakraborty, et al., Multiphonon longitudinal wobbling in  $^{127}\text{Xe}$ , *Phys. Lett. B* 811 (2020) 135854, <https://doi.org/10.1016/j.physletb.2020.135854>, <https://www.sciencedirect.com/science/article/pii/S0370269320306572>.
- [16] N. Sensharma, et al., Longitudinal wobbling motion in  $^{187}\text{Au}$ , *Phys. Rev. Lett.* 124 (2020) 052501, <https://doi.org/10.1103/PhysRevLett.124.052501>.
- [17] S. Nandi, et al., First observation of multiple transverse wobbling bands of different kinds in  $^{183}\text{Au}$ , *Phys. Rev. Lett.* 125 (2020) 132501, <https://doi.org/10.1103/PhysRevLett.125.132501>.
- [18] F.-Q. Chen, C.M. Petrache, Microscopic investigation on the existence of transverse wobbling under the effect of rotational alignment: The  $^{136}\text{Nd}$  case, *Phys. Rev. C* 103 (2021) 064319, <https://doi.org/10.1103/PhysRevC.103.064319>.
- [19] T.M. Semkow, et al., Spectroscopic study of the high-spin states in  $^{135}\text{Pr}$ , *Phys. Rev. C* 34 (1986) 523–535, <https://doi.org/10.1103/PhysRevC.34.523>.
- [20] S. Guo, <http://arxiv.org/abs/2011.14364>, to be published.
- [21] R. Garg, et al., Negative-parity high-spin states and a possible magnetic rotation band in  $^{135}\text{Pr}_{76}$ , *Phys. Rev. C* 92 (2015) 054325, <https://doi.org/10.1103/PhysRevC.92.054325>.
- [22] K. Tanabe, K. Sugawara-Tanabe, Stability of the wobbling motion in an odd-mass nucleus and the analysis of  $^{135}\text{Pr}$ , *Phys. Rev. C* 95 (2017) 064315, <https://doi.org/10.1103/PhysRevC.95.064315>.
- [23] S. Guo, C.M. Petrache, <http://arxiv.org/abs/2007.10031v2>, to be published.
- [24] R. Garg, et al., *Phys. Rev. C* 100 (2019) 069901(E), <https://doi.org/10.1103/PhysRevC.100.069901>.
- [25] K. Tanabe, K. Sugawara-Tanabe, Reply to “comment on ‘stability of the wobbling motion in an odd-mass nucleus and the analysis of  $^{135}\text{Pr}$ ’”, *Phys. Rev. C* 97 (2018) 069802, <https://doi.org/10.1103/PhysRevC.97.069802>.
- [26] A.A. Raduta, R. Poenaru, C.M. Raduta, New approach for the wobbling motion in the even-odd isotopes  $^{161,163,165,167}\text{Lu}$ , *Phys. Rev. C* 101 (2020) 014302, <https://doi.org/10.1103/PhysRevC.101.014302>.
- [27] E.A. Lawrie, O. Shirinda, C.M. Petrache, Tilted precession and wobbling in triaxial nuclei, *Phys. Rev. C* 101 (2020) 034306, <https://doi.org/10.1103/PhysRevC.101.034306>.
- [28] B.F. Lv, et al., Tilted precession bands in  $^{135}\text{Nd}$ , *Phys. Rev. C* 103 (2021) 044308, <https://doi.org/10.1103/PhysRevC.103.044308>.
- [29] K. Starosta, et al., Experimental test of the polarization direction correlation method (pdco), *Nucl. Instrum. Methods Phys. Res., Sect. A* 423 (1) (1999) 16–26, [https://doi.org/10.1016/S0168-9002\(98\)01220-0](https://doi.org/10.1016/S0168-9002(98)01220-0), <https://www.sciencedirect.com/science/article/pii/S0168900298012200>.
- [30] A. Krämer-Flecken, et al., *Nucl. Instrum. Methods Phys. Res., Sect. A* 275 (2) (1989) 333–339, [https://doi.org/10.1016/0168-9002\(89\)90706-7](https://doi.org/10.1016/0168-9002(89)90706-7), <http://www.sciencedirect.com/science/article/pii/0168900289907067>.
- [31] C. Droste, et al., Pdco: polarizational-directional correlation from oriented nuclei, *Nucl. Instrum. Methods Phys. Res., Sect. A* 378 (3) (1996) 518–525, [https://doi.org/10.1016/0168-9002\(96\)00426-3](https://doi.org/10.1016/0168-9002(96)00426-3), <https://www.sciencedirect.com/science/article/pii/0168900296004263>.
- [32] C.W. Beausang, et al., Measurements on prototype ge and bgo detectors for the eurogam array, *Nucl. Instrum. Methods Phys. Res., Sect. A* 313 (1) (1992) 37–49, [https://doi.org/10.1016/0168-9002\(92\)90084-H](https://doi.org/10.1016/0168-9002(92)90084-H), <https://www.sciencedirect.com/science/article/pii/016890029290084H>.
- [33] G. Duchêne, et al., The clover: a new generation of composite ge detectors, *Nucl. Instrum. Methods Phys. Res., Sect. A* 432 (1) (1999) 90–110, [https://doi.org/10.1016/S0168-9002\(99\)00277-6](https://doi.org/10.1016/S0168-9002(99)00277-6), <https://www.sciencedirect.com/science/article/pii/S0168900299002776>.
- [34] D. Radford, *Nucl. Instrum. Methods Phys. Res., Sect. A* 361 (1–2) (1995) 297–305, [https://doi.org/10.1016/0168-9002\(95\)00183-2](https://doi.org/10.1016/0168-9002(95)00183-2), <http://www.sciencedirect.com/science/article/pii/0168900295001832>.
- [35] D. Radford, *Nucl. Instrum. Methods Phys. Res., Sect. A* 361 (1–2) (1995) 306–316, [https://doi.org/10.1016/0168-9002\(95\)00184-0](https://doi.org/10.1016/0168-9002(95)00184-0), <http://www.sciencedirect.com/science/article/pii/0168900295001840>.
- [36] GASPWARE, <https://github.com/sztaylor89/GASPware-1>.
- [37] See Supplemental Material.
- [38] C.J. Chiara, et al., *Phys. Rev. C* 75 (2007) 054305, <https://doi.org/10.1103/PhysRevC.75.054305>.
- [39] A. Herzán, et al., *Phys. Rev. C* 92 (2015) 044310, <https://doi.org/10.1103/PhysRevC.92.044310>.
- [40] K. Starosta, et al., *Nucl. Instrum. Methods Phys. Res., Sect. A* 423 (1999) 16, [https://doi.org/10.1016/S0168-9002\(98\)01220-0](https://doi.org/10.1016/S0168-9002(98)01220-0).
- [41] P.B. Semmes, I. Ragnarsson, *World Scientific*, 1990.
- [42] J. Allmond, J. Wood, Empirical moments of inertia of axially asymmetric nuclei, *Phys. Lett. B* 767 (2017) 226–231, <https://doi.org/10.1016/j.physletb.2017.01.072>, <http://www.sciencedirect.com/science/article/pii/S0370269317300916>.